Analytical expression for the α-decay half-life and understanding the data including very long life-times and superheavy nuclei

Basudeb Sahu
Department of Physics, North Orissa University, Baripada 757003, India
(Received 27 July 2008; published 13 October 2008)

An analytically solvable composite potential that can closely reproduce the combined potential of an $\alpha +$ nucleus system consisting of attractive nuclear and repulsive electrostatic potentials is developed. The exact s-wave solution of the Schrödinger equation with this potential in the interior region and the outside Coulomb wave function are used to give a heuristic expression for the width or half-life of the quasibound state at the accurately determined resonance energy, called the Q value of the decaying system. By using the fact that for a relatively low resonance energy, the quasibound state wave function is quite similar to the bound state wave function where the amplitude of the wave function in the interaction region is very large as compared to the amplitude outside, the resonance energy could easily be calculated from the variation of relative probability densities of inside and outside waves as a function of energy. By considering recent α-decay systems, the applicability of the model is demonstrated with excellent explanations being found for the experimental data of Q values and half-lives of a vast range of masses including superheavy nuclei and nuclei with very long lifetimes (of order 10^{22} s). Throughout the application, by simply varying the value of a single potential parameter describing the flatness of the barrier, we obtain successful results in cases with as many as 70 pairs of $\alpha +$ daughter nucleus systems.

DOI: 10.1103/PhysRevC.78.044608 PACS number(s): 23.60.+e, 21.10.Tg, 27.90.+b

I. INTRODUCTION

Recent experiments on α decay [1–12] provide good precision data of Q values and decay half-lives for many $\alpha +$ daughter nucleus systems involving nuclei with proton number ranging from $Z = 52$ to 118. In these host of data listed in Ref. [13], there are results of decay half-lives as long as 10^{22} s, representing extremely long lived states. The explanation of these data has led to new theoretical studies on α decay, for example, within the relativistic mean-field theory [14] and using the density-dependent M3Y (DDM3Y) interaction [15,16], the generalized liquid drop model (GLDM) [17,18], the Skyrme-Hartree-Fock mean-field model [6], and phenomenological formulations [13,19]. If α emission from a parent nucleus is understood as a two-body quantum collision phenomenon involving the daughter and the parent nuclei, a proper theoretical approach to calculate Q values and half-lives requires a reliable input of α-daughter nucleus potential. By using the latest development in mean-field theory methods, many potentials for several pairs of α-daughter nucleus system have become available. Once such a potential is obtained, the α-decay process can be subjected to a quasi-molecular decay path, which is governed by a composite potential with a pocket followed by a barrier resulting from the combined effect of the repulsive Coulomb force and the attractive nuclear force. As a first step toward making a theoretical estimate of Q value and decay half-life, we may mention the well-known WKB type semiclassical approximation [20], where one obtains the energies of long-lived states of the effective potential. Then one evaluates the probability of decay of the α-daughter nucleus systems. The product of the constant assault frequency and the barrier penetrability calculated approximately by the WKB formula [20] gives the results of the decay constant and hence the mean life and half-life of decay. This method has certain problems related to the frequency factor [21].

However, the decaying state could be understood as the resonance state of the α-daughter nucleus two-body system within the framework of quantum scattering theory, where the resonance state is understood as a positive energy state with finite and relatively long lifetime or, equivalently, a narrow width. The most rigorous definition of a resonance state and its width can be obtained from the analytic S matrix (SM) theory of potential scattering. In this formulation, resonances are identified as poles of the SM in the lower half of the complex momentum ($k = \sqrt{2mE/\hbar^2}$ with energy E and reduced mass m) close to the real axis. The complex pole position $k = k_r - ik_i$ gives both energy [$E_r = \frac{\hbar^2}{2m}(k_r^2 - k_i^2)$] and width ($\Gamma = \frac{\hbar^2}{2m} 4k_r k_i$) of the resonance state. This approach has been applied to the study of resonances in several applications [20,22–24]. Though the SM method is rigorous in principle, it suffers from serious problems in searching the poles, particularly in the case of the α-nucleus system where we deal with the Coulomb-nuclear problem. As both the height and the spatial width of the potential barrier at the required Q value are quite large, the magnitude of the imaginary part (k_i) of the pole position ($k_r - ik_i$) is infinitesimally small (typically $\frac{k_i}{k_r}$ is 10^{-18} or less). Further, the S matrix has a zero at $k = k_r + ik_i$. Thus, the S matrix jumps from pole position to zero position very rapidly and creates serious problems in reaching saturation in the iterative process in the SM pole search method. Further, the irregular Coulomb wave function found in the expression to decide pole position of the s-wave Coulomb-nuclear S matrix takes exponentially large values and hence creates a problem in searching this pole.

In view of these difficulties in the numerical computation for resonance position and width in SM theory, we have to consider other quantal methods for the α-nucleus problem. In recent years methods have been developed [21,25–27] to calculate narrow widths or corresponding long half-lives for the decaying states by utilizing the behavior of these quasibound state wave functions (WFs). These methods are quite appropriate for the calculation of extremely narrow widths of decaying systems governed by the Coulomb-nuclear interaction. As the WF method depends critically on the nature of the wave functions, an unambiguous estimate of the wave function is essential in these calculations.

In this paper, we simulate the Coulomb-nuclear potential of the α-nucleus system by a versatile potential expressed with some parameters that account for the depth, range, diffuseness, flatness, position, and height of the resultant potential showing a pocket followed by a barrier. With this potential the s-wave Schrödinger equation is solved for the wave function. This exact wave function within the nuclear interaction region is properly matched with the pure Coulomb wave function found appropriate in the outer region of the barrier at a radial position within the barrier region and an analytical expression for the decay width or half-life is obtained as per the prescription of the WF method. We use the confinement property and the bound-state-like behavior of the wave function at the resonance state to estimate the energy of resonance or the Q value of the decaying state unambiguously. The corresponding decay half-life is calculated by straightforward computation of the analytical expression previously stated.

The formulation is applied to the simultaneous estimate of Q values and half-lives of a host of α-nucleus systems that include very heavy nuclei also. We need to fix the values of several potential parameters that describe the potential of the decaying system. These values may vary from system to system while bringing close agreement of the calculated results of Q values and half-lives with the respective measured data. However, we have been able to find a global set of values for these parameters, barring one parameter (λ_1) that accounts for the flatness of the barrier. Having fixed the values for all other parameters, we vary the value of the parameter λ_1 within a specified range $1 < \lambda_1 < 2$, enabling us to explain the data of all these systems or nuclei with remarkable success.

In Sec. II, we describe the potential used in the calculation and present the formulation for an analytical expression of the decay half-life. The experimental results of Q values and half-lives of several nuclei are explained quantitatively by our calculated results in Sec. III. Section IV contains the summary and conclusion.

II. FORMULATION

A. The potential

The proposed potential [23] as a function of radial variable r is given by

$$V(r) = \begin{cases} V_{01}\{\lambda_1^2[B_0 + (B_1 - B_0)(1 - y_1^2)] + \xi_1\} & \text{if} \quad 0 < r < R_1, \\ V_{02}\{\lambda_2^2 B_2(1 - y_2^2) + \xi_2\} & \text{if} \quad r \geqslant R_1, \end{cases} \tag{1}$$

where

$$\xi_1 = \left(\frac{1-\lambda_1^2}{4}\right)[5(1-\lambda_1^2)y_1^4 - (7-\lambda_1^2)y_1^2 + 2](1-y_1^2),$$

$$\xi_2 = \left(\frac{1-\lambda_2^2}{4}\right)[5(1-\lambda_2^2)y_2^4 - (7-\lambda_2^2)y_2^2 + 2](1-y_2^2).$$

Here, V_{01} and V_{02} are the strength of the potential in MeV. Denoting the mass of the particle moving under the potential by m, we use dimensionless variable $\rho_n = (r - R_1)b_n$ with $b_n = [(2m/\hbar^2)V_{0n}]^{1/2}$, $n = 1, 2$, such that ρ_n is related to the new variable y_n as

$$\rho_n = \frac{1}{\lambda_n^2}\left[\tanh^{-1} y_n - \left(1-\lambda_n^2\right)^{1/2} \tanh^{-1}\left(1-\lambda_n^2\right)^{1/2} y_n\right]. \tag{2}$$

The ranges of variation of r, ρ_n, and y_n are as follows. In the interior side r varies from 0 to R_1, ρ_1 varies from $-R_1 b_1$ to 0 while y_1 starts with a value close to -1 and ends up with zero at $r = R_1$. In the outer side, while r goes from R_1 to ∞, ρ_2 varies from 0 to ∞ and hence y_2 varies from 0 to 1.

The parameters λ_1, B_0, and B_1 specify the potential in the interior region $r < R_1$ and the parameters λ_2 and B_2 specify the potential in the outer region $r > R_1$. Equation (1) generates a potential barrier at $r = R_1$ or $y_1 = y_2 = 0$ with the height V_B of the barrier expressed as

$$V_B = V_{01}\left[\lambda_1^2 B_1 + \frac{1-\lambda_1^2}{2}\right] = V_{02}\left[\lambda_2^2 B_2 + \frac{1-\lambda_2^2}{2}\right], \tag{3}$$

so that $V_{01} = V_B/[\lambda_1^2 B_1 + (1-\lambda_1^2)/2]$ and $V_{02} = V_B/[\lambda_2^2 B_2 + (1-\lambda_2^2)/2]$.

The parameters λ_2 and B_2 control the flatness and range of the potential, respectively, in the region $r \geqslant R_1$, whereas the corresponding parameters in the left side ($r < R_1$) of the barrier are denoted by λ_1 and B_1. Near the origin ($r = 0$), the value of the potential is given by the quantity $V_{01}\lambda_1^2 B_0$ in MeV when V_{01} is in MeV. Thus the parameter B_0 is used to decide the magnitude of the potential near the origin, which can be positive or negative, and by this we can generate potential pockets of different depths in the region $0 < r \leqslant R_1$.

For a typical α-nucleus system with α particle as the projectile and the daughter nucleus as the target, let A_p and A_t denote mass numbers and Z_p and Z_t stand for charge numbers, respectively, with m representing the reduced mass of the system. One can use the following global expression for the

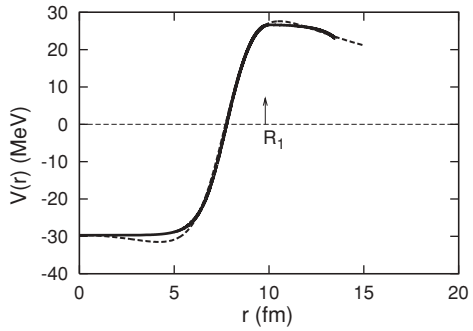

FIG. 1. Plot of potential $V(r)$ as a function of radial distance for the $\alpha + {}^{273}_{110}$Ds system. The dashed curve represents the sum of Coulomb and nuclear potential expressed by Eq. (6) with Woods-Saxon parameters $V_{N0} = -78.75$ MeV, $a_N = 0.84$ fm, $R_N = 7.649$ fm, and $R_C = 9.688$ fm. The solid curve represents the potential expressed by Eq. (1) in the text with parameters $\lambda_1 = 1.5987$, $B_0 = -78.75$, $B_1 = 21.2$, $\lambda_2 = 1$, $B_2 = 150$, $r_0 = 0.9$ fm, and $a = 1.6$ fm. The arrow indicates the barrier position R_1.

radial position R_1 and height V_B for the barrier potential [28]:

$$R_1 = r_0\left(A_p^{1/3} + A_t^{1/3}\right) + 2.72, \tag{4}$$

$$V_B = \frac{Z_p Z_t e^2}{R_1}\left(1 - \frac{a}{R_1}\right), \tag{5}$$

where r_0 and a are two distance parameters expressed in femtometers and $e^2 = 1.4398$ MeV fm. There are altogether seven parameters, namely, $\lambda_1, B_0, B_1, \lambda_2, B_2, r_0$, and a, to describe the total effective potential expressed by Eq. (1). Considering some values for these parameters, $\lambda_1 = 1.5987$, $B_0 = -78.75$, $B_1 = 21.2$, $\lambda_2 = 1$, $B_2 = 150$, $r_0 = 0.9$, fm and $a = 1.6$ fm with regard to the $\alpha + {}^{273}_{110}$Ds system, we plot the potential expressed by Eq. (1) as a solid curve in Fig. 1. As we can see, this potential having a pocket and a barrier resembles closely the sum total

$$V_T(r) = V_N(r) + V_C(r) \tag{6}$$

of nuclear (V_N) and Coulomb (V_C) potentials shown by a dashed curve in the short-range region $0 < r < R_1$, where $V_N(r)$ in Woods-Saxon form is

$$V_N(r) = -V_{N0}/\{1 + \exp[(r - R_N)/a_N]\}, \tag{7}$$

$$V_C(r) = \begin{cases} (Z_t Z_p e^2)\left(3R_C^2 - r^2\right)/\left(2R_C^3\right) & \text{if} \quad 0 < r < R_C, \\ (Z_t Z_p e^2)/r & \text{if} \quad r > R_C \end{cases} \tag{8}$$

with certain values of the parameters $V_{N0} = -78.75$ MeV, $a_N = 0.84$ fm, $R_N = 7.649$ fm, and $R_C = 9.688$ fm.

B. Solution

With the potential expressed by Eq. (1), the reduced Schrödinger equations for the s wave can be written in the dimensionless form as follows [23]:

$$-\frac{d^2u_1(\rho_1)}{d\rho_1^2} + \left\{\left[\lambda_1^2(B_1 - B_0)\left(1 - y_1^2\right) + \xi_1\right] - \frac{E_{\text{c.m.}}}{V_{01}} + \lambda_1^2(B_0)\right\}u_1(\rho_1) = 0, \quad r \leqslant R_1, \tag{9}$$

$$-\frac{d^2u_2(\rho_2)}{d\rho_2^2} + \left\{\left[\lambda_2^2 B_2\left(1 - y_2^2\right) + \xi_2\right] - \frac{E_{\text{c.m.}}}{V_{02}}\right\} \times u_2(\rho_2) = 0, \quad r > R_1. \tag{10}$$

Here, $E_{\text{c.m.}}$ stands for the incident center-of-mass energy. These equations can be solved analytically. The solution $u_1(\rho_1)$ in the region $r \leqslant R_1$ is given by

$$u_1(\rho_1) = A_1\left[\lambda_1^2 + \left(1 - \lambda_1^2\right)z_1^2\right]^{1/4}\left(1 - z_1^2\right)^{-\frac{ik_1}{2\lambda_1^2}} F \times \left(a_1, b_1, c_1, \frac{1 - z_1}{2}\right) + A_2\left[\lambda_1^2 + \left(1 - \lambda_1^2\right)z_1^2\right]^{1/4} \times \left(1 - z_1^2\right)^{\frac{ik_1}{2\lambda_1^2}} F\left(a_1', b_1', c_1', \frac{1 - z_1}{2}\right), \tag{11}$$

where the new variable

$$z_1 = \frac{\lambda_1 y_1}{\left[1 + \left(\lambda_1^2 - 1\right)y_1^2\right]^{1/2}},$$

$F(a, b, c, z)$ is the hypergeometric function, and

$$a_1 = \bar{\nu}_1 + 1 - \frac{ik_1}{\lambda_1^2}, \quad b_1 = -\bar{\nu}_1 - \frac{ik_1}{\lambda_1^2}, \quad c_1 = 1 - \frac{ik_1}{\lambda_1^2},$$

$$a_1' = \bar{\nu}_1 + 1 + \frac{ik_1}{\lambda_1^2}, \quad b_1' = -\bar{\nu}_1 + \frac{ik_1}{\lambda_1^2}, \quad c_1' = 1 + \frac{ik_1}{\lambda_1^2},$$

$$\bar{\nu}_1 = \left[\frac{1}{4} - (B_1 - B_0) + \frac{\lambda_1^2 - 1}{\lambda_1^4}k_1^2\right]^{1/2} - \frac{1}{2},$$

$$k_1^2 = \frac{E_{\text{c.m.}}}{V_{01}} - \lambda_1^2 B_0.$$

The solution $u_2(\rho_2)$ in the region $r > R_1$ is given by

$$u_2(\rho_2) = A_3\left[\lambda_2^2 + \left(1 - \lambda_2^2\right)z_2^2\right]^{1/4}\left(1 - z_2^2\right)^{\frac{-ik_2}{2\lambda_2^2}} F \times \left(a_2, b_2, c_2, \frac{1 - z_2}{2}\right) + A_4\left[\lambda_2^2 + \left(1 - \lambda_2^2\right)z_2^2\right]^{1/4} \times \left(1 - z_2^2\right)^{\frac{ik_2}{2\lambda_2^2}} F\left(a_2', b_2', c_2', \frac{1 - z_2}{2}\right), \tag{12}$$

where the variable

$$z_2 = \frac{\lambda_2 y_2}{\left[1 + \left(\lambda_2^2 - 1\right)y_2^2\right]^{1/2}}$$

and

$$a_2 = \bar{\nu}_2 + 1 - \frac{ik_2}{\lambda_2^2}, \quad b_2 = -\bar{\nu}_2 - \frac{ik_2}{\lambda_2^2}, \quad c_2 = 1 - \frac{ik_2}{\lambda_2^2},$$

$$a_2' = \bar{\nu}_2 + 1 + \frac{ik_2}{\lambda_2^2}, \quad b_2' = -\bar{\nu}_2 + \frac{ik_2}{\lambda_2^2}, \quad c_2' = 1 + \frac{ik_2}{\lambda_2^2},$$

$$\bar{\nu}_2 = \left[\frac{1}{4} - B_2 + \frac{\lambda_2^2 - 1}{\lambda_2^4}k_2^2\right]^{1/2} - \frac{1}{2},$$

$$k_2^2 = \frac{E_{\text{c.m.}}}{V_{02}}.$$

Near the origin $r = 0$, we have

$$\rho_1 = -R_1 b_1, \quad y_1 = y_{01} = -\left[1 - 2e^{2\lambda_1^2(\rho_{01}-|\rho_1|)}\right],$$
$$\rho_{01} = \frac{\left(\lambda_1^2-1\right)^{1/2}}{\lambda_1^2} \arctan\left(\lambda_1^2-1\right)^{1/2},$$
$$z_1 = z_{01} = \frac{\lambda_1 y_{01}}{\left[1+\left(\lambda_1^2-1\right)y_{01}^2\right]^{1/2}}.$$

The boundary condition

$$u_1(\rho_1) \to 0 \text{ for } r \to 0$$

gives us

$$C_1 = -\frac{A_2}{A_1} = \left(1-z_{01}^2\right)^{-i\kappa_1} \frac{F\left(a_1, b_1, c_1, \frac{1-z_{01}}{2}\right)}{F\left(a_1', b_1', c_1', \frac{1-z_{01}}{2}\right)}, \quad (13)$$

where $\kappa_1 = \frac{k_1}{\lambda_1^2}$ and

$$F\left(a_1, b_1, c_1, \frac{1-z_{01}}{2}\right) = \frac{\Gamma(1-i\kappa_1)\Gamma(i\kappa_1)}{\Gamma(-\bar{\nu}_1)\Gamma(1+\bar{\nu}_1)} + \left(\frac{1+z_{01}}{2}\right)^{i\kappa_1} \times \frac{\Gamma(1-i\kappa_1)\Gamma(-i\kappa_1)}{\Gamma(\bar{\nu}_1+1-i\kappa_1)\Gamma(-\bar{\nu}_1-i\kappa_1)}, \quad (14)$$

$$F\left(a_1', b_1', c_1', \frac{1-z_{01}}{2}\right) = \frac{\Gamma(1+i\kappa_1)\Gamma(-i\kappa_1)}{\Gamma(-\bar{\nu}_1)\Gamma(1+\bar{\nu}_1)} + \left(\frac{1+z_{01}}{2}\right)^{-i\kappa_1} \times \frac{\Gamma(1+i\kappa_1)\Gamma(i\kappa_1)}{\Gamma(\bar{\nu}_1+1+i\kappa_1)\Gamma(-\bar{\nu}_1+i\kappa_1)}, \quad (15)$$

$$\left(1-z_{01}^2\right)^{-i\kappa_1} \simeq \exp\left\{(-2ik_1)\left(\frac{1}{\lambda_1^2}\log 2 - \frac{1}{\lambda_1^2}\log\lambda_1 + \rho_{01} - b_1 R_1\right)\right\}, \quad (16)$$

$$\left(\frac{1+z_{01}}{2}\right)^{i\kappa_1} \simeq \exp\left\{(-2ik_1)\left(\frac{1}{\lambda_1^2}\log\lambda_1 - \rho_{01} + b_1 R_1\right)\right\}. \quad (17)$$

The property of the wave function $u_2(\rho_2)$ for large $\rho_2 \to \infty$ (or $r \to \infty$) gives

$$u_2 = A_4 2^{\frac{ik_2}{\lambda_2^2}} e^{-ik_2\rho_2'}[e^{-ik_2\rho_2} - S_m e^{ik_2\rho_2}] \quad \text{for } \rho_2 \to \infty, \quad (18)$$

where the scattering matrix denoted by S_m is expressed as

$$S_m = C_2 \exp\left[(-2ik_2)\left(\frac{\log 2}{\lambda_2^2} - \rho_2'\right)\right], \quad (19)$$

with

$$C_2 = -\frac{A_3}{A_4}, \qquad \rho_2' = \frac{1}{\lambda_2^2}\log\lambda_2 - \rho_{02}, \quad (20)$$

and

$$\rho_{02} = \frac{\left(\lambda_2^2-1\right)^{1/2}}{\lambda_2^2} \arctan\left(\lambda_2^2-1\right)^{1/2}.$$

Equating the logarithmic derivatives of $u_1(\rho_1)$ and $u_2(\rho_2)$ at $\rho_1 = \rho_2 = 0$, we can calculate C_2 and hence the scattering matrix S_m.

For the Coulomb-nuclear problem, the potential in the region $r > R_1$ can be considered pure Coulombic and the outer solution $u_2(\rho_2)$ in this analysis can be replaced by the Coulomb-distorted outgoing spherical wave $f_C(kr) = G_0(\eta, kr) + iF_0(\eta, kr)$ for the s wave. Here, with the reduced mass m, the wave number $k = \sqrt{(2m/\hbar^2)E_{\text{c.m.}}}$, η stands for the Coulomb parameter $\eta = mZ_pZ_te^2/\hbar^2k$, and $F_0(\eta, kr)$ and $G_0(\eta, kr)$ are the regular and irregular Coulomb wave functions, respectively.

C. Resonance energy

The potential given by Eq. (1), having a pocket followed by a repulsive barrier as shown in Fig. 1, generates quasibound states with discrete positive energies called resonance energies. One of these energies is recognized as the Q value for the decaying system with some lifetime for decay. Exactly at a resonance energy, the wave function looks like a bound-state wave function depicting the confinement property that the probability density ($I = \int |u|^2 dr$) in the interior region ($0 < r < R_1$) is very large as compared to that in the outer region ($r > R_1$). If the energy under consideration is slightly different from the exact resonance energy, these results of densities of the inner and outer wave functions get reversed. This behavior of the wave function is shown in Figs. 2(a) and 2(b) in the case of a typical $\alpha + {}^{273}_{100}$Hs system at and near the resonance energy $E_{\text{c.m.}} = 11.618$ MeV. We calculate the results of probability densities in two regions:

(i) from $r = 0$ to $r = R_1$, $I_1 = \int_0^{R_1} |u|^2 dr$, and
(ii) from $r = 0$ to $r = R_2$ with $R_2 > R_1$, $I_2 = \int_0^{R_2} |u|^2 dr$.

Comparing these two densities, in Fig. 3 we plot the ratio $I_r = \frac{I_1}{I_2}$ as a function of incident energy. The plot shows a sharp peak at the exact resonance energy, which is easily identified and recorded as the Q value of the system. We call this method of calculating resonance energy the relative probability density (RPD) method, which is found to be clean and free from any ambiguities or difficulties experienced in other methods, namely, (i) searching of poles of the S matrix in the complex energy plane [20,22], (ii) variation of reaction cross section using test imaginary potential [22], (iii) variation of phase-shift time as a function of energy in the phase-shift method [22], and (iv) the WKB approximation [20].

D. Decay lifetime or width of resonance

For the calculation of width or lifetime of the resonance state, we follow the procedure presented in Ref. [25] where one uses the wave functions on either side of the matching radius $r = R_1$. The normalized regular solution $u_1(r)$ of the modified Schrödinger equation is matched at $r = R_1$ to the distorted outgoing Coulomb wave,

$$u_1(R_1) = N_0\,[G_0(\eta, kR_1) + iF_0(\eta, kR_1)], \quad (21)$$

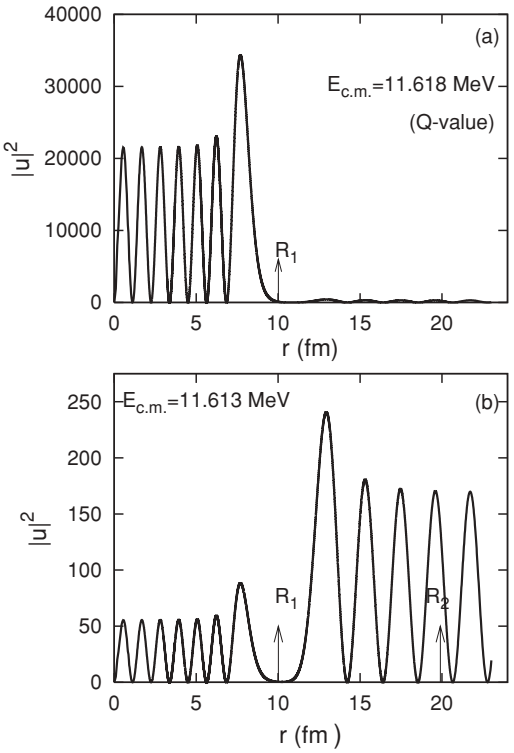

FIG. 2. Plot of the square modulus of the wave function as a function of radial distance r for the $\alpha + {}^{273}_{110}$Ds system (a) at the resonance energy $E_{\text{c.m.}} = 11.618$ MeV, called the Q value, and (b) at an energy $E_{\text{c.m.}} = 11.613$ MeV, less than resonance energy by 0.005 MeV. R_1 stands for barrier position and R_2 indicates a position in the outer region $r > R_1$.

where R_1 is outside the range of the nuclear field. Calculating radial probability flux through a sphere by using the radial wave function on the right-hand side of Eq. (21) and following Ref. [26], one can express the mean lifetime τ (or width Γ) of decay in terms of matching amplitude N_0 as

$$\tau = \frac{\hbar}{\Gamma} = \frac{m}{\hbar k}\frac{1}{|N_0|^2}. \tag{22}$$

Since the wave function $u_1(r)$ decreases rapidly with radius outside the nucleus, it can be normalized by requiring

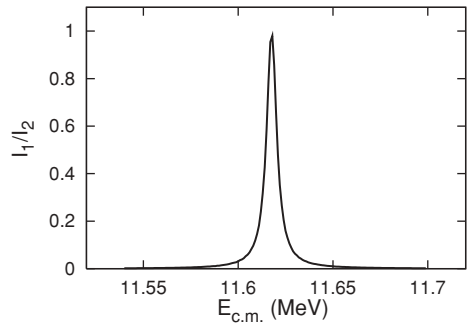

FIG. 3. Plot of the ratio of probability densities I_1 and I_2 (see text) as a function of energy $E_{\text{c.m.}}$ for the $\alpha + {}^{273}_{110}$Ds system. The peak position ($E_{\text{c.m.}} = 11.618$ MeV) represents the resonance energy (Q value).

that

$$\int_0^{R_1} |u_1(r)|^2 dr = 1, \tag{23}$$

where $R_1 < R_2$, R_2 being a large distance close to the classical outermost turning point. It should be noted that unlike the normalization of bound state, this normalization is confined to the interior domain $r \leqslant R_1$. Using this normalized $u_1(r)$, one gets

$$N_0 = \frac{u_1(R_1)}{G_0(\eta, kR_1) + iF_0(\eta, kR_1)}. \tag{24}$$

In our analysis, $u_1(R_1)$ is the wave function [Eq. (11)] $u_1(r) = A_1\tilde{u}_1(r)$ calculated at $r = R_1$, where $\tilde{u}_1(r)$ at $r = R_1$ can be expressed explicitly as

$$\tilde{u}_1(R_1) = \lambda_1^{1/2} F\left(a_1, b_1, c_1, \frac{1}{2}\right) - C_1\lambda_1^{1/2} F\left(a_1', b_1', c_1', \frac{1}{2}\right), \tag{25}$$

$$F\left(a_1, b_1, c_1, \frac{1}{2}\right) = \pi^{1/2}\frac{\Gamma(1 - i\kappa_1)}{\Gamma\left(\frac{\bar{\nu}_1}{2} - \frac{i\kappa_1}{2} + 1\right)\Gamma\left(-\frac{\bar{\nu}_1}{2} - \frac{i\kappa_1}{2} + \frac{1}{2}\right)}, \tag{26}$$

$$F\left(a_1', b_1', c_1', \frac{1}{2}\right) = \pi^{1/2}\frac{\Gamma(1 + i\kappa_1)}{\Gamma\left(\frac{\bar{\nu}_1}{2} + \frac{i\kappa_1}{2} + 1\right)\Gamma\left(-\frac{\bar{\nu}_1}{2} + \frac{i\kappa_1}{2} + \frac{1}{2}\right)}, \tag{27}$$

where $C_1(= -A_2/A_1)$ is expressed by Eq. (13) and $A_1 = (\int_0^{R_1} |\tilde{u}_1(r)|^2 dr)^{-1/2}$ is obtained through the normalization of Eq. (23).

In the special cases of the Coulomb-nuclear problem, there are specific values for η, k, and R_1 for which $F_0(\eta, kR_1)$ and $G_0(\eta, kR_1)$ can be expressed approximately. In the case where $2\eta > kR_1$ for $\ell = 0$ [29],

$$F_0(\eta, kR_1) \approx \frac{1}{2}\beta e^{\gamma}, \quad G_0(\eta, kR_1) \approx \beta e^{-\gamma}, \quad t = \frac{kR_1}{2\eta},$$
$$\gamma = 2\eta\left\{[t(1-t)]^{\frac{1}{2}} + \sin^{-1} t^{\frac{1}{2}} - \frac{1}{2}\pi\right\}, \tag{28}$$
$$\beta = \{t/(1-t)\}^{\frac{1}{2}}.$$

Further, in this condition of $2\eta > kR_1$, one finds that $|G_0(\eta, kR_1)| \gg |F_0(\eta, kR_1)|$ by several orders of magnitude. This condition prevails in the α-nucleus systems of interaction at energies below the respective Coulomb barrier height and hence Eq. (24) can be reduced to

$$N_0 \simeq \frac{u_1(R_1)}{G_0(\eta, kR_1)}. \tag{29}$$

By using Eq. (25) for $u_1(R_1)$ and Eq. (28) for $G_0(\eta, kR_1)$ in Eq. (29), N_0 is calculated at a given energy and it is used in Eq. (22) for the final result of mean life τ (or half-life $\tau_{1/2} = 0.693\tau$) of the decay process at the same energy (the so-called Q value).

The correctness of our RPD method of calculation of resonance energy and the analytical expression [Eq. (22)] for

width can be demonstrated in the cases of the two similar potentials shown in Fig. 1. For the Coulomb nuclear potential shown by the dashed curve and expressed by Eq. (6), the S matrix is obtained by numerical (Runge-Kutta) integration of the Schrödinger equation and the pole of this S matrix searched and found in the complex k-plane gives resonance energy $E_r = 11.618$ MeV and width $\Gamma = 9.66 \times 10^{-18}$ MeV. Using the potential expressed by Eq. (1) and shown by the solid curve in Fig. 1, one finds that the resonance energy calculated by the RPD method is equal to 11.618 MeV and the result of the width calculated by using Eq. (29) in Eq. (22) is found to be $\Gamma = 3.67 \times 10^{-18}$ MeV. This is exactly the same resonance energy as calculated previously by a pole of the S matrix, and the width is fairly close to the previously calculated value given by a pole of the S matrix as well. Hence, one can use, with confidence, the RPD method for calculating resonance energy and Eq. (22) along with Eq. (29) for decay lifetime (τ) for a decaying system with a potential expressed through Eq. (1). In the following section, we apply this formulation to a number of α + nucleus systems for an explanation of the experimental results of Q values and α-decay half-lives.

III. RESULTS AND DISCUSSION

The application of the formulation described in Sec. II requires an input potential for the α + nucleus system, which is obtained recently by calculations based on mean-field theoretic methods [20]. Such a potential for the $\alpha + {}^{273}_{110}$Ds system [30] is closely reproduced by our analytically solvable potential [Eq. (1)] by fixing the values of five potential parameters, namely, r_0, a, B_0, $b_1 = \sqrt{B_1} A_t^{-1/3}$, and λ_1 for the estimate of resonance energy (Q value) and the corresponding half-life $\tau_{1/2}$. To obtain the results for a variety of systems involving light and heavy masses, the values of these parameters may require some changes for a close agreement with the respective experimental data of different systems. However, in the whole of our application, we vary the value of one and only one parameter: λ_1, which describes flatness of the barrier within the range $1 < \lambda_1 < 2$. The values of remaining four parameters are fixed at $r_0 = 0.97$ fm, $a = 1.6$ fm, $B_0 = -78.75$, and $b_1 = 0.82$. We, first, using the RPD method, obtain the exact experimental Q value as the resonance energy for certain value of λ_1. With the same value of λ_1 and calculated Q value, we obtain the result of $\tau_{1/2} = 0.693\tau$ by using Eq. (22) along with Eq. (29) and denote it by $\tau_{1/2}^{(\text{formula})}$. These results together with the experimental Q value ($Q^{(\text{expt})}$) and the half-life $\tau_{1/2}^{(\text{expt})}$ are presented in Tables I, II, and III for various α + daughter nucleus systems obtained from Ref. [13].

It is clearly seen in Tables I and II that there is quite good agreement between our calculated results and the corresponding experimental data of half-lives in the

TABLE I. Comparison between recently known experimental results [13] of α-decay half-lives and results of present calculation. Values of potential parameters $r_0 = 0.97$ fm, $a = 1.6$ fm, $b_1 = 0.82$, and $B_0 = -78.75$ are the same for all nuclei except for ^{174}Hf, where $r_0 = 1.1$ fm and $b_1 = 1.085$. Only the value of the parameter λ_1 is varied (by the amount shown in parentheses under the respective nucleus).

Nucleus	$Q^{(\text{expt})}$ (MeV)	$\tau_{1/2}^{(\text{expt})}$ (s)	$\tau_{1/2}^{(\text{formula})}$ (s)
^{105}Te (1.04004)	4.900(0.050)	$0.70^{+0.25}_{-0.17} \times 10^{-6}$	$0.50^{+0.28}_{-0.18} \times 10^{-6}$
^{158}Yb (1.04009)	4.172	4.3×10^{6}	4.3×10^{6}
^{174}Hf (1.011391)	2.497	6.3×10^{22}	32.5×10^{22}
^{168}W (1.04839)	4.507	1.6×10^{6}	4.8×10^{6}
^{164}Os (1.18718)	6.475	4.2×10^{-2}	2.1×10^{-2}
^{168}Pt (1.23205)	6.997	2.0×10^{-3}	2.0×10^{-3}
^{172}Hg (1.27918)	7.525	4.2×10^{-4}	2.6×10^{-4}
^{188}Hg (1.06521)	4.705	5.3×10^{8}	4.0×10^{8}
^{180}Pb (1.27963)	7.415	5.0×10^{-3}	2.9×10^{-3}
^{186}Pb (1.21065)	6.470	1.2×10^{1}	0.60×10^{1}
^{190}Pb (1.14380)	5.697	1.8×10^{4}	1.3×10^{4}
^{194}Pb (1.05386)	4.738	9.8×10^{9}	2.7×10^{9}
^{156}Er (1.005184)	3.486	2.3×10^{10}	3.8×10^{10}
^{160}Hf (1.08179)	4.902	1.9×10^{3}	2.3×10^{3}
^{158}W (1.21285)	$6.612^{+0.003}_{-0.003}$	$1.5^{+2}_{-2} \times 10^{-3}$	$1.1^{+0.02}_{-0.01} \times 10^{-3}$
^{162}Os (1.20250)	$6.767^{+0.003}_{-0.003}$	$1.9^{+2}_{-2} \times 10^{-3}$	$2.0^{+0.04}_{-0.03} \times 10^{-3}$
^{166}Pt (1.24814)	7.286	3.0×10^{-4}	2.6×10^{-4}
^{170}Pt (1.21581)	6.708	1.4×10^{-2}	1.9×10^{-2}
^{174}Hg (1.261133)	7.233	2.1×10^{-3}	2.0×10^{-3}
^{178}Pb (1.313420)	7.790	2.3×10^{-4}	2.2×10^{-4}
^{184}Pb (1.231678)	6.774	6.1×10^{-1}	4.2×10^{-1}
^{188}Pb (1.180780)	6.109	2.7×10^{2}	1.8×10^{2}
^{192}Pb (1.09850)	5.221	3.6×10^{6}	3.6×10^{6}
^{188}Po (1.41747)	$8.087^{+0.025}_{-0.025}$	$4.0^{+2.0}_{-1.5} \times 10^{-4}$	$1.5^{+0.18}_{-0.14} \times 10^{-4}$

TABLE II. Comparison between recently known experimental results [13] of α-decay half-lives and results of present calculation. Values of potential parameters $r_0 = 0.97$ fm, $a = 1.6$ fm, $b_1 = 0.82$, and $B_0 = -78.75$ are the same for all nuclei. Only the value of the parameter λ_1 is varied (by the amount shown in parentheses under the respective nucleus).

Nucleus	$Q^{(\text{expt})}$ (MeV)	$\tau_{1/2}^{(\text{expt})}$ (s)	$\tau_{1/2}^{(\text{formula})}$ (s)
^{189}Po (1.36152)	$7.703^{+0.020}_{-0.020}$	$5.0^{+1}_{-1} \times 10^{-3}$	$2.0^{+0.19}_{-0.16} \times 10^{-3}$
^{192}Po (1.33788)	$7.319^{+0.011}_{-0.011}$	$2.9^{+1.5}_{-0.8} \times 10^{-2}$	$3.1^{+0.16}_{-0.2} \times 10^{-2}$
^{196}Rn (1.34243)	$7.616^{+0.009}_{-0.009}$	$4.4^{+1.3}_{-0.9} \times 10^{-3}$	$18.9^{+0.09}_{-0.08} \times 10^{-3}$
^{202}Ra (1.39686)	8.020	2.6×10^{-3}	5.5×10^{-3}
^{210}Th (1.41015)	8.053	1.7×10^{-2}	2.1×10^{-2}
^{218}U (1.56564)	$8.773^{+0.009}_{-0.009}$	$5.1^{+1.7}_{-1.0} \times 10^{-4}$	$8.8^{+0.37}_{-0.28} \times 10^{-4}$
^{224}U (1.63331)	8.620	7.0×10^{-4}	22.7×10^{-4}
^{228}Pu (1.42281)	7.950	2.0×10^{-1}	11.0×10^{-1}
^{238}Cm (1.19663)	6.62	2.3×10^{5}	7.7×10^{5}
^{258}Rf (1.51164)	9.25	9.2×10^{-2}	3.1×10^{-1}
^{266}Hs (1.61460)	10.34	2.3×10^{-3}	7.1×10^{-3}
^{270}Ds (1.75789)	11.2	1.0×10^{-4}	2.7×10^{-4}
^{190}Po (1.37532)	7.693	2.5×10^{-3}	2.1×10^{-3}
^{210}Po (1.25548)	5.407	1.2×10^{7}	0.30×10^{7}
^{198}Rn (1.32403)	7.349	6.5×10^{-2}	13.9×10^{-2}
^{204}Ra (1.35477)	7.636	5.9×10^{-2}	8.6×10^{-2}
^{212}Th (1.42118)	7.952	3.6×10^{-2}	4.4×10^{-2}
^{220}U (1.99700)	10.30	6.0×10^{-8}	20.0×10^{-8}
^{226}U (1.46388)	7.701	5.0×10^{-1}	14.0×10^{-1}
^{230}Pu (1.30217)	7.180	1.0×10^{2}	5.9×10^{2}
^{258}No (1.40278)	8.151	1.2×10^{2}	1.6×10^{2}
^{260}Rf (1.46317)	8.901	1.0×10^{0}	3.2×10^{0}
^{270}Hs (1.368)	9.02	2.2×10^{1}	2.7×10^{1}
^{282}113 (1.5708)	$10.63^{+0.08}_{-0.08}$	$7.3^{+13.4}_{-2.9} \times 10^{-2}$	$3.2^{+0.65}_{-1.82} \times 10^{-2}$

whole mass range. Graphically, such good agreement is demonstrated in Fig. 4 in the cases of different isotopes of the Pb nucleus. It may be mentioned here that there are cases (namely, ^{174}Hf, ^{156}Er, ^{194}Pb, ^{188}Hg, ^{210}Po, etc.) where the results of $\tau_{1/2}^{(\text{expt})}$ are very large, corresponding to very small widths in energy units. For instance, in the case of ^{156}Er, $\tau_{1/2}^{(\text{expt})} = 2.3 \times 10^{10}$ s corresponds to an experimental width $\Gamma^{(\text{expt})} = 1.98 \times 10^{-32}$ MeV. Such a small width could be reproduced by our calculation with $\tau_{1/2}^{(\text{formula})} = 3.8 \times 10^{10}$ s (see Table I), which corresponds to width $\Gamma^{(\text{formula})} = 1.2 \times 10^{-32}$ MeV. More exciting is the case of ^{174}Hf, which records an extremely long half-life of $\tau_{1/2}^{(\text{expt})} = 6.3 \times 10^{22}$ s, corresponding to width $\Gamma^{(\text{expt})} = 7.0 \times 10^{-45}$ MeV with the lowest measured Q value, $Q^{(\text{expt})} = 2.497$ MeV, in the whole mass region considered in the paper. Our calculation for this case gives $\tau_{1/2}^{(\text{formula})} = 32.5 \times 10^{22}$ s and $\Gamma^{(\text{formula})} = 1.4 \times 10^{-45}$ MeV. In this case we have used $r_0 = 1.1$ fm and $b_1 = 1.085$, which are slightly different from the respective values used in all other cases listed in Tables I, II, and III. As we see, our calculated results are very close to the measured results and this success in explaining such data of extremely small width or long decay time can be considered highly remarkable in the theoretical study of decay process.

Good agreement is also obtained in the cases of the heaviest elements presented in Table III where the uncertainties both in experimental Q values and α-decay half-lives are large. Lower and upper limits of the calculated half-lives ($\tau_{1/2}^{(\text{formula})}$), corresponding, respectively, to upper and lower limits of the experimental Q values, are also given. Besides very close fitting of the data, in some cases we have obtained

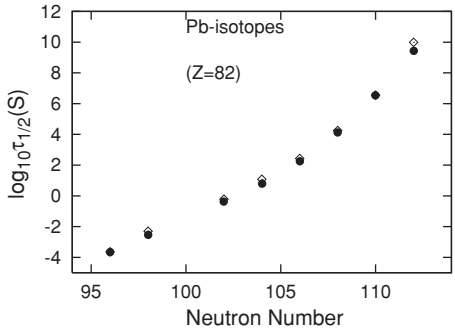

FIG. 4. α-decay half-lives for diffent isoptopes of the Pb nucleus. Solid dots represent calculated results using Eq. (22) along with Eq. (29) (see text). Experimental results (open diamonds) are obtained from Table I of Ref. [13].

TABLE III. Comparison between recently known experimental results [13] of α-decay half-lives and results of present calculation. Values of potential parameters $r_0 = 0.97$ fm, $a = 1.6$ fm, $b_1 = 0.82$, and $B_0 = -78.75$ are the same for all nuclei. Only the value of the parameter λ_1 is varied (see the last column).

Nucleus	$Q^{(\text{expt})}$ (MeV)	$\tau_{1/2}^{(\text{expt})}$	$\tau_{1/2}^{(\text{formula})}$	λ_1
^{294}118	11.81 ± 0.06	$1.8^{+7.5}_{-1.3}$ ms	$1.7^{+0.4}_{-0.3}$ ms	1.68738
^{293}116	10.67 ± 0.06	53^{+62}_{-19} ms	213^{+69}_{-46} ms	1.52691
^{292}116	10.80 ± 0.07	18^{+16}_{-6} ms	101^{+34}_{-25} ms	1.543823
^{291}116	10.89 ± 0.07	$6.3^{+11.5}_{-2.5}$ ms	61^{+22}_{-13} ms	1.55048
^{290}116	11.0 ± 0.08	15^{+26}_{-6} ms	33^{+14}_{-8} ms	1.56231
^{288}115	10.61(6)	87^{+105}_{-30} ms	157^{+49}_{-31} ms	1.50840
^{287}115	10.74(9)	32^{+155}_{-14} ms	75^{+36}_{-20} ms	1.52475
^{289}114	9.96 ± 0.06	$2.7^{+1.4}_{-0.7}$ s	$3.9^{+1.4}_{-0.90}$ s	1.44146
^{288}114	10.09 ± 0.07	$0.8^{+0.32}_{-0.18}$ s	$1.7^{+0.70}_{-0.45}$ s	1.45700
^{287}114	10.16 ± 0.06	$0.51^{+0.18}_{-0.10}$ s	$1.1^{+0.39}_{-0.25}$ s	1.45828
^{286}114	10.35 ± 0.06	$0.16^{+0.07}_{-0.03}$ s	$0.36^{+0.12}_{-0.08}$ s	1.48850
^{284}113	10.15(6)	$0.48^{+0.58}_{-0.17}$ s	$0.62^{+0.19}_{-0.15}$ s	1.48336
^{283}113	10.26(9)	100^{+490}_{-45} ms	317^{+162}_{-100} ms	1.49422
^{285}112	9.29 ± 0.06	34^{+17}_{-9} s	82^{+34}_{-22} s	1.37139
^{283}112	9.67 ± 0.06	$4.0^{+1.3}_{-0.7}$ s	$6.3^{+2.3}_{-1.6}$ s	1.50132
^{280}111	9.87(6)	$3.6^{+4.3}_{-1.3}$ s	$0.88^{+0.29}_{-0.21}$ s	1.50132
^{279}111	10.52(6)	170^{+810}_{-80} ms	$19^{+20}_{-6.5}$ ms	1.65069
^{279}110	9.84 ± 0.06	$0.18^{+0.05}_{-0.03}$ s	$0.53^{+0.17}_{-0.12}$ s	1.55289
^{276}109	9.85(6)	$0.72^{+0.87}_{-0.25}$ s	$0.24^{+0.07}_{-0.06}$ s	1.58232
^{275}109	10.48(9)	$9.7^{+46}_{-4.4}$ ms	$6.6^{+3.0}_{-1.5}$ ms	1.73313
^{275}108	9.44 ± 0.07	$0.15^{+0.27}_{-0.06}$ s	$1.6^{+0.78}_{-0.35}$ s	1.53931
^{272}107	9.15(6)	$9.8^{+11.7}_{-3.5}$ s	$5.5^{+2.03}_{-1.29}$ s	1.49537
^{271}106	8.65 ± 0.08	$2.4^{+4.3}_{-1.9}$ min	$1.5^{+0.9}_{-0.48}$ min	1.43561

results slightly more and in other cases slightly less than the corresponding experimental data, but on average, the explanation of the data is satisfactory. The explanation in individual cases can be improved further, provided the values of r_0, b_1, and hence λ_1 are slightly varied. To maintain consistency, we have not changed the values of r_0 (= 0.97 fm) and b_1 (=0.82) in the whole analysis of all masses presented in Tables I, II, and III, barring the unique case of ^{174}Hf.

We may conclude here that by the variation of the value of a single parameter λ_1 within a well-defined range $1 < \lambda_1 < 2$ (see Tables I, II, and III), we have obtained the results of Q value and α-decay half-lives that are close to the respective experimental data in the whole mass range from $A = 105$ ($Z = 52$) to $A = 294$ ($Z = 118$) recently presented in Ref. [13].

In the process of achieving this success in explaining the experimental data of α-decay half-lives and Q value, we have obtained the following systematics with regard to the nature of the three crucial parameters λ_1, b_1, and r_0 that describe the property of the effective potential barrier that critically governs the decay process:

(i) By increasing the value of r_0, the same resonance energy equal to the measured Q value can be obtained by some minor changes in the values of λ_1 and b_1. However, the result of half-life $\tau_{1/2}$ for larger r_0 is smaller than the value corresponding to smaller r_0.

(ii) For a given value of r_0, the same Q value can be obtained in two different ways: (a) by using small λ_1 with larger b_1 and (b) by using larger λ_1 with smaller b_1. However, unlike the Q value, the results of $\tau_{1/2}$ in these two situations are not same. Rather, in situation (a), the calculated result, $\tau_{1/2}^{(\text{formula})}$, is slightly less than that of experiment, $\tau_{1/2}^{(\text{expt})}$, whereas in the latter case (b) $\tau_{1/2}^{(\text{formula})} \geqslant \tau_{1/2}^{(\text{expt})}$. Following this nature of λ_1 and b_1, we see that further variations of these parameters would lead to a result almost equal to $\tau_{1/2}^{(\text{expt})}$ at the measured Q value.

IV. SUMMARY AND CONCLUSION

The phenomenon of decay of an α particle from a parent nucleus is analyzed within the framework of potential scattering problem of an α + daughter nucleus system. In such a system, the attractive short-range nuclear force and the long-range electrostatic force combine to generate a potential that shows a pocket near the origin and a barrier outside. This composite potential is simulated by a versatile and realistic potential with a pocket and a barrier for which an exact expression for the s-wave S matrix is analytically derivable. The functional form of the potential is such that one can readily vary its parameters to generate different forms for the pocket and the barrier to closely reproduce the α + nucleus potential. This potential generates discrete positive-energy quasibound states called resonance states. One of these states is recognized as the α-decay state, with its Q value being equal to the resonance energy and its decay half-life related to the width of the resonance state. Using the confinement property of the wave function at the resonance state one can calculate the exact resonance energy. After matching the interior wave function with the outside pure Coulomb wave function, an analytical expression for the width or decay half-life of the resonance state is presented.

The formulation is applied to several α + nucleus systems starting from a nucleus with $A = 105$ ($Z = 52$) to a nucleus with $A = 294$ ($Z = 118$) to explain recent experimental data of Q values and half-lives. Having reproduced exactly the measured Q values, we can explain the respective measured half-lives by our calculated results with remarkable success. In this process of explaining the Q-value and half-life data simultaneously for the whole mass region stated, the following important features emerge:

(i) By the variation of a single parameter (λ_1) that describes the flatness of the potential barrier within a specified range $1 < \lambda_1 < 2$, the results of the whole mass region including superheavy nuclei could be explained.

(ii) By using an analytical expression for the decay half-life, the measured results of very long half-lives (2.3×10^{10} s in the case of α + ^{156}Er and 6.3×10^{22} s for α + ^{174}Hf, which correspond to the extremely narrow resonance

widths of order 10^{-32} and 10^{-45} MeV, respectively) are explained quite accurately by our calculated results. This success in explaining the extremely narrow width is believed to be a remarkable achievement in this fully quantum mechanical description of the decay process.

The formulation can be applied to the explanation of experimental results of half-lives of spherical proton emitters. This will be reported soon.

ACKNOWLEDGMENTS

The author is grateful to Prof. C. S. Shastry and Prof. Y. K. Gambhir for fruitful discussion and encouragement for the development of the analytical formulation for the α-decay process. He thanks Prof. Y. K. Gambhir for providing potential data based on mean-field theory. This work is supported by the Department of Science and Technology (DST), New Delhi, India, via Research Grant No. SR/S2/HEP-18/2004.

[1] Yu. Ts. Oganessian *et al*., Phys. Rev. C **69**, 021601(R) (2004); **69**, 054607 (2004); **70**, 064609 (2004).
[2] Yu. Ts. Oganessian *et al*., Phys. Rev. C **71**, 029902(E) (2005); **72**, 034611 (2005); **74**, 044602 (2006).
[3] S. Hofmann *et al*., Eur. Phys. J. A **32**, 251 (2007).
[4] Yu. Ts. Oganessian *et al*., Phys. Rev. C **76**, 011601(R) (2007).
[5] K. Morita *et al*., J. Phys. Soc. Jpn. **76**, 045001 (2007).
[6] J. C. Pei, F. R. Xu, Z. J. Lin, and E. G. Zhao, Phys. Rev. C **76**, 044326 (2007).
[7] A. N. Andreyev *et al*., Eur. Phys. J. A **6**, 381 (1999).
[8] F. Garcia, O. Rodriguez, M. Goncalves, S. B. Duarte, O. A. P. Tavares, and F. Guzman, J. Phys. G: Nucl. Part. Phys. **26**, 755 (2000).
[9] H. Mahmud *et al*., Phys. Rev. C **62**, 057303 (2000).
[10] H. Kettunen *et al*., Phys. Rev. C **63**, 044315 (2001).
[11] D. Seweryniak *et al*., Phys. Rev. C **73**, 061301(R) (2006).
[12] A. P. Leppänen *et al*., Phys. Rev. C **75**, 054307 (2007).
[13] G. Royer and H. F. Zhang, Phys. Rev. C **77**, 037602 (2008).
[14] M. M. Sharma, A. R. Farhan, and G. Münzenberg, Phys. Rev. C **71**, 054310 (2005).
[15] D. N. Basu, J. Phys. G: Nucl. Part. Phys. **30**, B 35 (2004).
[16] P. R. Chowdhury, D. N. Basu, and C. Samanta, Phys. Rev. C **75**, 047306 (2007).
[17] H. F. Zhang, W. Zuo, J. Q. Li, and G. Royer, Phys. Rev. C **74**, 017304 (2006).
[18] H. F. Zhang and G. Royer, Phys. Rev. C **76**, 047304 (2007).
[19] R. Moustabchir and G. Royer, Nucl. Phys. **A683**, 266 (2001).
[20] S. Mahadevan, P. Prema, C. S. Shastry, and Y. K. Gambir, Phys. Rev. C **74**, 057601 (2006).
[21] S. Aberg, P. B. Semmes, and W. Nazarewicz, Phys. Rev. C **56**, 1762 (1997); **58**, 3011 (1998).
[22] B. Sahu, L. Satpathy, and C. S. Shastry, Phys. Lett. **A303**, 105 (2002).
[23] B. Sahu, G. S. Mallick, and S. K. Agarwalla, Nucl. Phys. **A727**, 299 (2003).
[24] B. Sahu, B. M. Jyrwa, P. Susan, and C. S. Shastry, Phys. Rev. C **44**, 2729 (1991).
[25] C. N. Davids and Henning Esbensen, Phys. Rev. C **61**, 054302 (2000).
[26] E. Maglione, L. S. Ferreira, and R. J. Liotta, Phys. Rev. Lett. **81**, 538 (1998).
[27] V. P. Bugrov, S. G. Kadmensky, V. I. Furman, and V. G. Khelbostroev, Sov. J. Nucl. Phys. **41**, 717 (1985).
[28] R. A. Broglia and A. Winther, *Heavy-Ion Reactions Lecture Notes* (Addison-Wesley, Redwood City, CA, 1981), p. 116.
[29] M. Abramowitz and I. A. Stegun, *Handbook of Mathematical Functions* (Dover, New York, 1965), p. 542.
[30] Y. K. Gambhir (private communication, 2008).